Stem Cell Reports
Article

ISSCR

OPEN ACCESS

Comparative RNAi Screens in Isogenic Human Stem Cells Reveal *SMARCA4* as a Differential Regulator

Ceren Güneş,[1] Maciej Paszkowski-Rogacz,[1] Susann Rahmig,[2] Shahryar Khattak,[3] Aylin Camgöz,[1,9] Martin Wermke,[4,5] Andreas Dahl,[6] Martin Bornhäuser,[4] Claudia Waskow,[2,7] and Frank Buchholz[1,8,9,10,*]

[1]Medical Faculty and University Hospital Carl Gustav Carus, UCC Section Medical Systems Biology, TU Dresden, 01307 Dresden, Germany
[2]Regeneration in Hematopoiesis, Leibniz Institute on Aging – Fritz Lipmann Institute, 07745 Jena, Germany
[3]Stem Cell Engineering Facility, Biotechnology Center, TU Dresden, 01307 Dresden, Germany
[4]Department of Medicine I, University Hospital Carl Gustav Carus, 01307 Dresden, Germany
[5]Medical Faculty and University Hospital Carl Gustav Carus, Early Clinical Trial Unit, 01307 Dresden, Germany
[6]Dresden Genome Center (DGC), TU Dresden, 01307 Dresden, Germany
[7]Department of Medicine III, Faculty of Medicine, Fetscherstrasse 74, 01307 Dresden, Germany
[8]German Cancer Research Center (DKFZ), Heidelberg and German Research Consortium (DKTK), Partner Site Dresden, 01307 Dresden, Germany
[9]National Center for Tumor Diseases (NCT), University Hospital Carl Gustav Carus, TU Dresden, 01307 Dresden, Germany
[10]Max Planck Institute of Molecular Cell Biology and Genetics, 01307 Dresden, Germany
*Correspondence: frank.buchholz@tu-dresden.de
https://doi.org/10.1016/j.stemcr.2019.03.012

SUMMARY

Large-scale RNAi screens are a powerful approach to identify functions of genes in a cell-type-specific manner. For model organisms, genetically identical (isogenic) cells from different cell types are readily available, making comparative studies meaningful. However, large-scale screens in isogenic human primary cells remain challenging. Here, we show that RNAi screens are possible in genetically identical human stem cells, using induced pluripotent stem cells as intermediates. The screens revealed *SMARCA4* (SWI/SNF-related matrix-associated actin-dependent regulator of chromatin subfamily A member 4) as a stemness regulator, while balancing differentiation distinctively for each cell type. *SMARCA4* knockdown in hematopoietic stem and progenitor cells caused impaired self-renewal *in vitro* and *in vivo* with skewed myeloid differentiation; whereas, in neural stem cells, it impaired self-renewal while biasing differentiation toward neural lineage, through combinatorial SWI/SNF subunit assembly. Our findings pose a powerful approach for deciphering human stem cell biology and attribute distinct roles to *SMARCA4* in stem cell maintenance.

INTRODUCTION

Stem cells have been in the focus of regenerative medicine because of their two key features: self-renewal and differentiation (Daley et al., 2003; Keller, 2005). Great progress has been made in the stem cell field since the discovery of induced pluripotent stem cells (iPSCs) in mice (Takahashi and Yamanaka, 2006) and in humans (Takahashi et al., 2007; Yu et al., 2007). This discovery paved numerous paths including disease modeling and derivation and expansion of somatic stem cells such as hematopoietic stem and progenitor cells (HSPCs) (Sugimura et al., 2017) or neural stem cells (NSCs) (Reinhardt et al., 2013). Although both HSPCs and NSCs are among the most extensively studied human adult stem cells, it has been challenging to understand the molecular basis behind self-renewal and differentiation, in particular in a comparative way. Interestingly, genes and pathways involved in the fine-tuning of self-renewal and differentiation are often shown to be key players in tumorigenesis (Orkin and Zon, 2008), which renders stem cell research crucial and indispensable in multiple aspects.

Development of RNAi technology has transformed the pace of functional genetics and provided tools for genome-wide screens. Importantly, RNAi screens have also been performed on mammalian stem cell lines (Ding et al., 2011; Elling and Penninger, 2014; Moffat and Sabatini, 2006) and on patient-derived cells (Camgoz et al., 2018; Wermke et al., 2015) and can be customized for the purpose of each study. Several studies have dissected genetic regulations in human HSPCs by lentiviral short hairpin RNA (shRNA) libraries. For instance, *STK38* (Ali et al., 2009), *MAPK14* (Baudet et al., 2012), and cohesin genes (Galeev et al., 2016) have been identified as modifiers of HSPC self-renewal and differentiation. In contrast, NSCs have not been studied in this context, despite being among the most widely studied adult stem cells. Moreover, no comparative study to our knowledge has been performed to identify which genes or regulators function in common, or in a cell-type-specific manner in these stem cells.

Ideally, comparative RNAi screens on human stem cells should be performed with isogenic cells, as only isogenic cells can provide an unbiased view for comparative analyses. To address the differences between multiple stem cells that are genetically identical, we hypothesized that cell fate determination is regulated by epigenetic factors. To this end, we chose to study HSPCs and NSCs, using iPSCs as a bridging cell type, and screened these stem cells with the identical shRNA library targeting 538 epigenetic factors. We identified *SMARCA4*, a chromatin remodeler

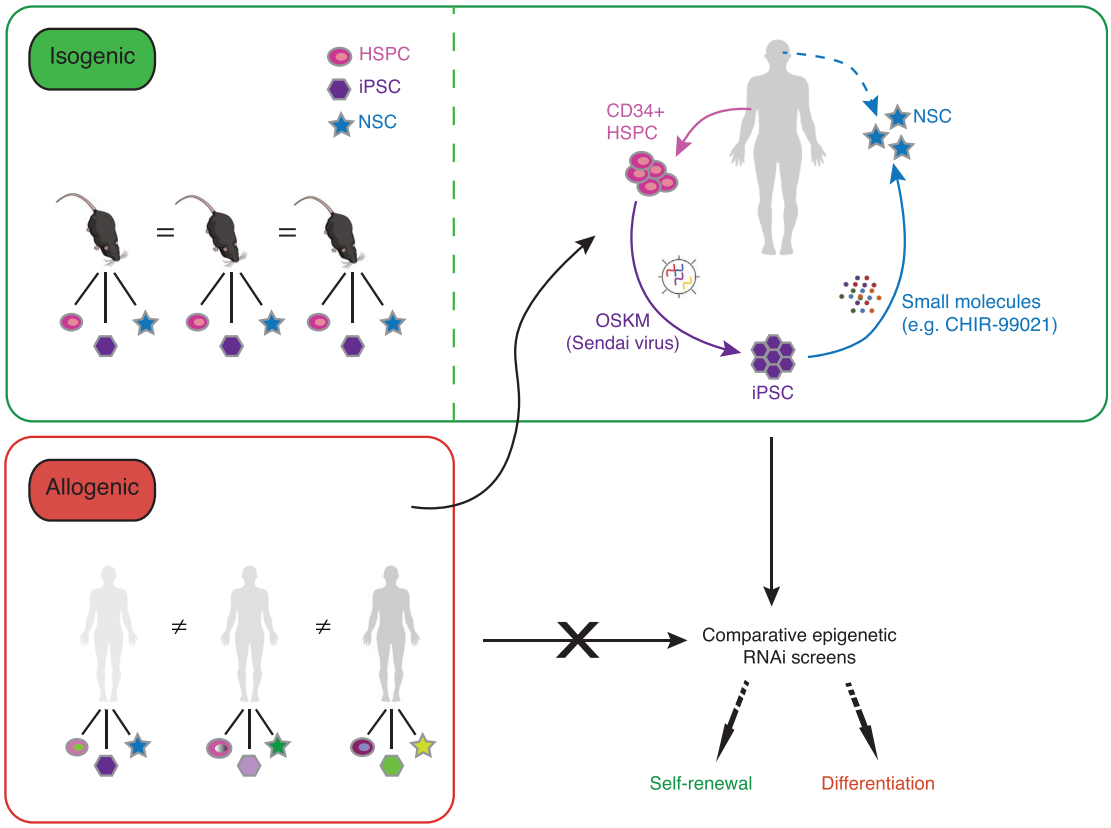

Figure 1. Schematic Representation of Comparative RNAi Screens on Isogenic Human Stem Cells

An alternative approach to derive isogenic stem cells from humans versus model organisms to perform large-scale screens in a comparative manner. Reprogramming of PB-derived CD34$^+$ HSPCs to iPSCs (bridging cell type) enables differentiation into NSCs. Dashed lines depict direct derivation of NSCs from human brain. Cells derived by reprogramming followed by differentiation serve as isogenic to the starting cell population. HSPC, hematopoietic stem and progenitor cell; iPSC, induced pluripotent stem cell; NSC, neural stem cell.

(Peterson and Tamkun, 1995), as a differential regulator of self-renewal/differentiation with cell-type-specific functions.

RESULTS

Isogenic Human Stem Cell Derivation via iPSCs

To be able to perform comparative RNAi screens on human stem cells, we derived isogenic human stem cells starting from peripheral blood (PB) of a healthy donor. HSPCs were isolated from PB using MACS-based sorting for CD34$^+$ cells and these cells were directly used for the RNAi screen. By using iPSCs as an intermediate cell type we derived isogenic NSCs, which all together provided the basis for unbiased screens (Figure 1).

Before performing the HSPC RNAi screen, we tested seven different suspension culture conditions to find condition boosting CD34$^+$ cell proliferation (increasing cell number) while keeping differentiation minimal (CD34$^+$ %). We tested conditions, including commercially available small molecules such as pyrimidoindole agonists, i.e., *UM171* (Fares et al., 2014, 2017) and *UM729* (Pabst et al., 2014), as well as cytokines at high concentrations. Addition of UM729 yielded the highest CD34$^+$ cell number at minimal differentiation during a 15-day cultivation period (Figure S1). Therefore, we included UM729 for all the following HSPC suspension culture experiments.

As a means of deriving isogenic cell types, we used iPSCs, which have been used as a source for numerous stem and terminally differentiated cells. While reprogramming HSPCs, we opted for a "zero-footprint" method using the Sendai virus, so that downstream experiments, including RNAi screens and NSC derivation, would not be affected by random genomic integration of the reprogramming factors. We established two iPSC lines, which were fully characterized before NSC derivation by iPSC-specific marker expression as well as by the three germ-layer differentiation potential (Figure S2). Next, we induced iPSC lines into NSCs by using a cocktail of small molecules (Reinhardt

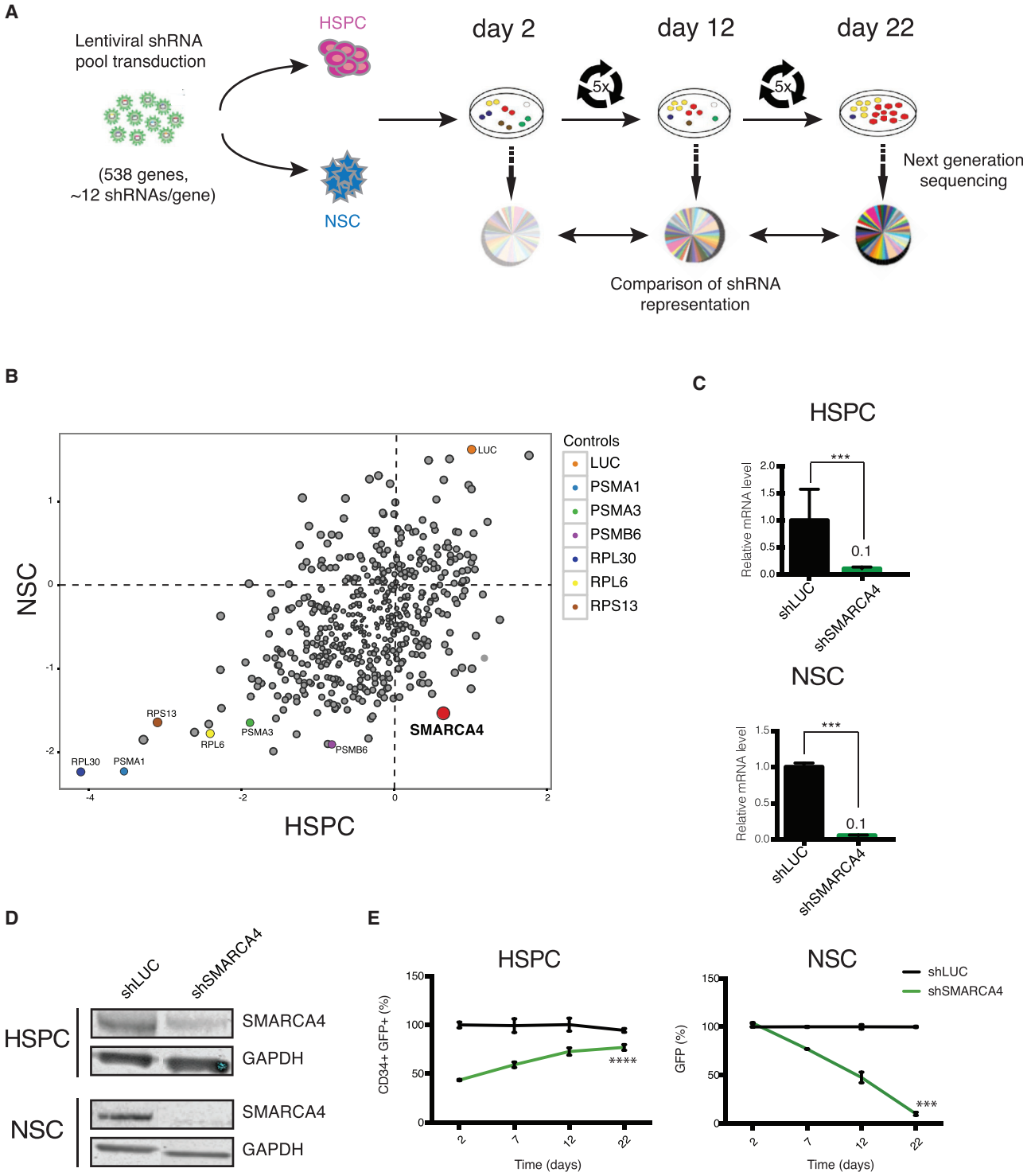

Figure 2. RNAi Screens Identify *SMARCA4* as a Hit with Divergent Phenotypes

(A) Screen strategy and timeline for the pooled shRNA screens. 5x in circled arrows represents 5 population doublings.

(B) Comparative analysis of the HSPC- and NSC-RNAi screens. Each dot represents a gene with the mean *Z* score of all targeting shRNAs. *SMARCA4* (enriched in HSPC versus depleted in NSC screen) is depicted in red. Positive controls and the negative control (LUC) are highlighted. See also Table S2.

(C) mRNA levels of *SMARCA4* upon knockdown in HSPCs (top) and NSCs (bottom) measured by qRT-PCR (n = 3).

(legend continued on next page)

et al., 2013). Loss of pluripotency was confirmed together with the concomitant upregulation of NSC-specific markers. In addition, similar to the iPSCs, we confirmed the functionality of NSCs by differentiation into neurons, astrocytes, and oligodendrocytes (Figure S3). To validate the isogenic nature of the iPSCs and the NSCs, we investigated the isogeneity of these cells by a short-tandem repeat analysis, which revealed their DNA profiles to be identical to the HSPC population (Table S1). Finally, we performed RNA sequencing (RNA-seq) experiments of the HSPCs, iPSCs, and NSCs, to compare their expression profile with published data (Chu et al., 2016; MacRae et al., 2013). As expected, our $CD34^+$ expression profile clustered with two different primary $CD34^+$ expression profiles; iPSCs with two embryonic stem cell (ESC) lines; and NSCs with two neural progenitor cell lines from the literature (Figure S3D). Taken together, we successfully established a minimally invasive approach to derive isogenic human stem cells for unbiased RNAi screens.

RNAi Screens Identify *SMARCA4* as a Differential Hit

To decipher cell fate determinants in isogenic cells, we used a pooled lentiviral shRNA library targeting epigenetic regulators. This library consists of 6,482 shRNAs and targets 538 genes—whereby each gene is typically targeted by 12 different shRNAs. As negative controls, 20 non-targeting shRNAs were included (*Renilla* Luciferase [LUC]), whereas 6 ribosomal and proteosomal genes served as positive controls (7 shRNAs/gene). We collected the first sample 2 days post transduction (dpt), which served as the baseline for comparison of shRNA representation to later time points. We allowed five population doublings between the time points and collected the second time point on 12 dpt, and the third time point sample on 22 dpt. To be able to trace phenotypes back to individual shRNAs, we ensured single shRNA integration by transducing each cell type at low MOI with at least a 150-fold coverage of the library. From each time point, genomic DNA was isolated from the cells and PCR-amplified fragments covering the shRNA sequences were subjected to next-generation sequencing (NGS) to identify how shRNA representation changed over time (Figure 2A; Table S2).

The screen results showed that the positive control shRNAs were depleted, whereas the negative control shRNAs displayed a relative enrichment phenotype (compared with the depleted shRNAs), rendering the screen successful. To evaluate the screen readout, it is important to remember that enrichment of shRNAs of a particular gene can be either due to enhanced self-renewal and cell proliferation or blocked differentiation, and vice versa for a depletion phenotype. Among the hits identified, we decided to investigate *SMARCA4* further because it displayed a variant phenotype. Indeed, knockdown of *SMARCA4* resulted in enrichment of shRNA reads in HSPCs, whereas in NSCs shRNAs targeting *SMARCA4* were depleted (Figure 2B), suggesting that this gene might have differential roles in these stem cell types.

SMARCA4 is one of the two core enzymatic subunits of the SWI/SNF complex, which is generally associated with 10–12 subunits of BRG1-associated factors (BAFs). As a core subunit, SMARCA4 has ATPase and helicase activities. The ATPase activity provides the energy via ATP hydrolysis, and the helicase activity unwinds the DNA strands with this energy to alter chromatin accessibility and regulate transcription (Trotter and Archer, 2008). SMARCA4 has been shown to act as a transcriptional activator and repressor, and, hence, has versatile functions (Attanasio et al., 2014).

Initially, we validated the screen results for the respective cell types by transducing cells with a *SMARCA4* shRNA, which had a *Z* score of less than –2 if depleted, and greater than +2 if enriched (Table S2). For the validation, we first confirmed the knockdown both at mRNA (~90% knockdown efficiency) (Figure 2C) and protein level (Figure 2D). Then, we took a similar approach as in the screen, and monitored the transduced cells for 22 days, based on the shRNA reporter marker expression (additionally with CD34 for HSPCs). We were able to reproduce the screen phenotypes, in which *SMARCA4* shRNA-transduced cells were enriched over time in HSPCs, whereas they were depleted in NSCs (Figure 2E). These data provided evidence that *SMARCA4* is a valid hit from the pooled RNAi screens.

SMARCA4 Knockdown Impairs HSPC Self-Renewal and Skews Differentiation

Results from the large-scale screen and the initial validation suggested that knockdown of *SMARCA4* increases the percentage of $CD34^+$ HSPCs over time. To validate this finding, we monitored the change in $CD34^+$ cell number as well as in the overall GFP percentage on *SMARCA4* knockdown. We observed that $CD34^+$ expression was retained in the knockdown cells, which led to a relative enrichment compared with the control. In addition, not only the $CD34^+$ percentage, but also the overall cell number, increased upon *SMARCA4* knockdown (Figure 3A, left). In addition, we also observed an increase in total percent of GFP, regardless

(D) Confirmation of the SMARCA4 knockdown at protein level by western blot. GAPDH served as loading control.
(E) Validation of screen phenotypes. Enrichment in HSPCs based on $CD34^+GFP^+$ expression (left) and depletion in NSCs based on GFP^+ cells (right). Values are normalized to day 2 control sample (HSPC) or shLUC at each time point (NSC).
Data from three independent experiments are represented as mean ± SEM. ***p < 0.001, ****p < 0.0001. See also Figures S1–S3.

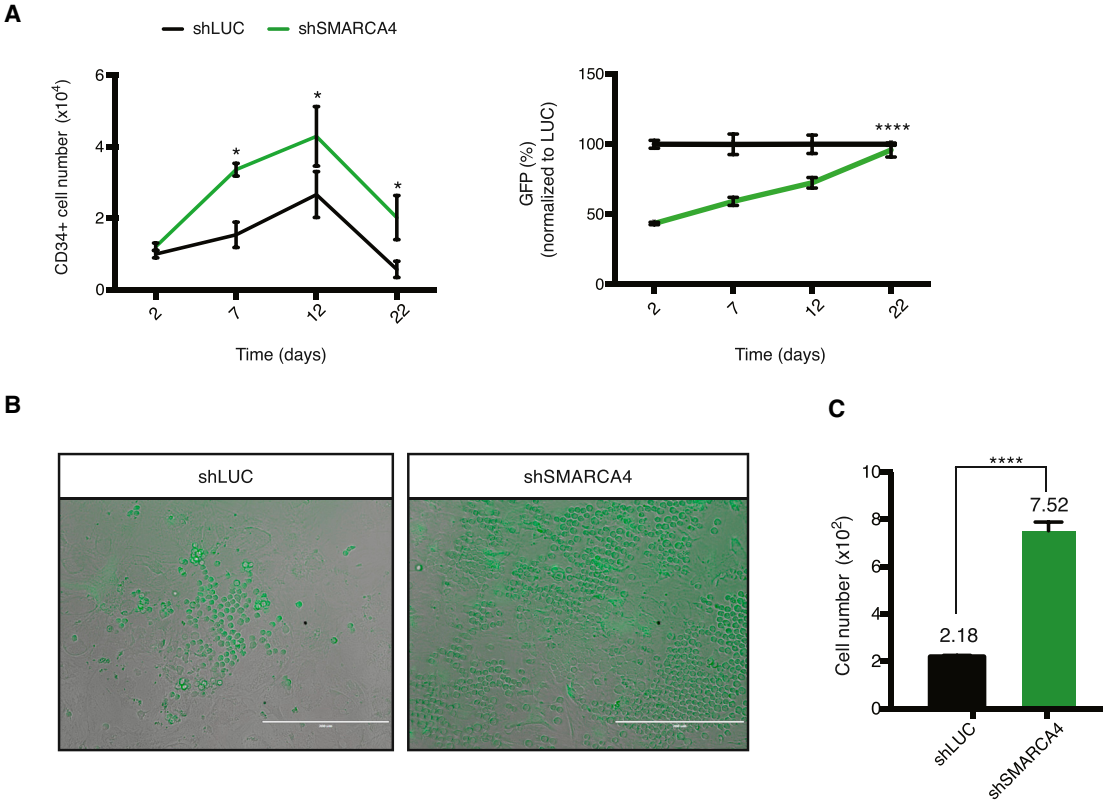

Subset	Markers
HSC	**CD34**+CD38-CD45RA-CD90+CD49f+
MPP	**CD34**+CD38-CD45RA-CD90-CD49f-
CLP	**CD34**+CD38-/loCD45RA+ CD90-
CMP	**CD34**+CD38+CD45RA-

(legend on next page)

of CD34 expression (Figure 3A, right). Therefore, we investigated further whether this enrichment is specific to HSPCs and whether *SMARCA4* has an effect on self-renewal. First, we examined HSPC functionality upon knock down by the long-term cell-initiating culture (LTC-IC) assay (Petzer et al., 1996). After 5 weeks of co-culturing shRNA-transduced HSPCs (GFP^+) with stromal feeder cells, substantially more GFP^+ cells were observed in the shSMARCA4-transduced cells compared with the control (Figure 3B), and *SMARCA4* knockdown led to higher overall cell numbers (3.5-fold, Figure 3C). These data support our previous findings and together can explain the enrichment phenotype observed in the HSPC screen.

We then evaluated the readout of the LTC-IC assay by cobblestone formation, which indicates the frequency and activity of HSPCs. As of week 2, cobblestone emergence was observed in both shSMARCA4- and control-transduced groups. However, despite higher cell numbers in suspension, *SMARCA4* knockdown cells showed a substantial reduction in cobblestone formation (Figure 3D). Thus, *SMARCA4* depletion results in higher $CD34^+$ cell number, but this increase is not due to enhanced self-renewal of HSPCs.

To investigate this observation in more detail, we addressed how *SMARCA4* affects cell differentiation. To this end, we analyzed different hematopoietic subsets in suspension culture, based on immune phenotypes: HSC, multipotent progenitor (MPP), common lymphoid progenitor (CLP), and common myeloid progenitor (CMP), both derived from MPP (Akashi et al., 2000; Kondo et al., 1997; Notta et al., 2011). Of note, all these cell populations express CD34. Interestingly, *SMARCA4* knockdown resulted in significant reduction of the phenotypically similar HSC and MPP populations; whereas both CLP and CMP showed an increase by 4- and 32-fold, respectively (Figure 3E).

To test whether differentiation capacity is altered upon *SMARCA4* knockdown, we performed colony-forming unit (CFU) assays, in which cells are cytokine induced to form colonies of myeloid origin. At 2 weeks of culture, we noted a significant reduction in overall colony numbers. Moreover, *SMARCA4* knockdown samples gave rise only to CFU-GM (granulocyte-macrophage), whereas no erythroid colony formation was observed (Figure 3F). Together, these data suggest that *SMARCA4* depletion in HSPCs leads to reduced self-renewal and an imbalanced differentiation toward the myeloid lineage *in vitro*.

SMARCA4 Knockdown Impedes *In Vivo* Engraftment of HSPCs

We next investigated how *SMARCA4* knockdown affects hematopoiesis *in vivo*. To be able to evaluate the change in percentage of the GFP^+ cells, we transplanted (5×10^5) HSPCs that were infected at a 30%–35% transduction rate with either shSMARCA4 or shLUC into NSGW41 mice (Cosgun et al., 2014) (Figure 4A). To investigate the long-term HSCs (LT-HSCs), we analyzed mice 6 months after transplantation (Zon, 2008). On bone marrow (BM) analysis of the engrafted human cells ($hCD45^+$), engraftment rates of GFP^+ cells were strikingly low on *SMARCA4* knockdown (Figure 4B). These results indicate that *SMARCA4* is essential for LT-HSC maintenance, and consequently for hematopoiesis.

On the one hand, our findings show that *SMARCA4* knockdown leads to exit from self-renewal and impedes engraftment *in vivo*; on the other hand, it directs differentiation to progenitors of both myeloid and lymphoid lineages, however, with less capacity of further myeloid differentiation. Altogether, *SMARCA4* is an important regulator of hematopoiesis as its loss leads to impaired self-renewal together with expansion of $CD34^+$ cells and distorted differentiation *in vitro* and impeded engraftment *in vivo*.

Figure 3. *SMARCA4* Knockdown Phenotypes in HSPCs

(A) Increase in $CD34^+$ cell number (left) and GFP^+ percentage (right) upon *SMARCA4* depletion. Values are normalized to day 2 sample (left) or shLUC at each time point (right). Data from three independent experiments are represented as mean ± SEM.

(B) LTC-IC assay week 5. shRNA-transduced HSPCs (GFP^+) cells are shown on the M2-10B4 feeder cells for indicated treatments. Note the increased number of GFP^+ cells in the shSMARCA4-treated sample. Scale bars, 200 μm.

(C) Quantification of the GFP^+ cell numbers. Data from three replicates are presented as mean ± SEM. Note the increase in cell number in the shSMARCA4-treated sample.

(D) Number of cobblestones in LTC-IC assay between weeks 2 and 5. Data from two independent experiments are represented as mean ± SEM (n = 5).

(E) Immunophenotyping of GFP^+ hematopoietic subsets with the indicated marker combination 5 days post shRNA transduction. All subsets analyzed express CD34. Data from three independent experiments are represented as mean ± SEM. HSC, hematopoietic stem cell; MPP, multipotent progenitor; CLP, common lymphoid progenitor; CMP, common myeloid progenitor.

(F) Colony-forming unit (CFU) assay. Colonies were imaged 14 days after seeding. Data from three independent experiments are represented as mean ± SEM (n = 3). M, macrophage; E, erythroid; CFU-GEMM, CFU-granulocyte, erythrocyte, macrophage, megakaryocyte; CFU-GM, CFU-granulocyte, macrophage; BFU-E, burst-forming unit-erythrocyte.

*p < 0.05, **p < 0.01, ***p < 0.001, ****p < 0.0001.

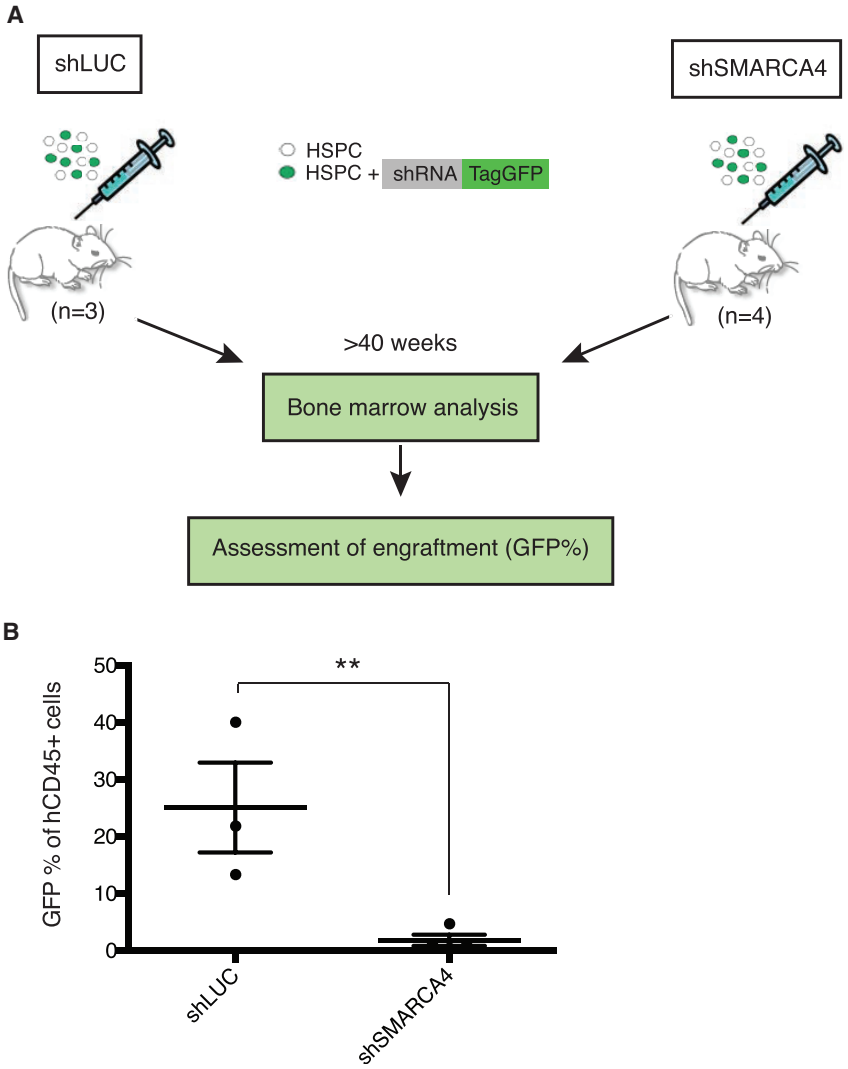

Figure 4. *SMARCA4* Depletion Impairs HSC Engraftment *In Vivo*

(A) Schematic representation of the transplantation experiment. NSGW41 mice injected with 5×10^5 HSPCs carrying the control (n = 3 mice) and *SMARCA4* shRNA (n = 4 mice). Bone marrow was analyzed >40 weeks after transplantation.

(B) Engraftment based on GFP percentage of the hCD45 cells in the control (n = 3) versus *SMARCA4* shRNA-transplanted mice (n = 4). **p < 0.01; n.s., not significant.

Loss of Self-Renewal and Cell Detachment in NSCs

In contrast to the enrichment of shRNAs targeting *SMARCA4* in the HSC screen, the same shRNAs were depleted in the NSC screen (Figure 2B). To validate the screen phenotype in NSCs, we transduced NSCs with lentiviral particles expressing *SMARCA4* shRNAs in conjunction with GFP and monitored the cells over time by fluorescence microscopy. Strikingly, we observed a very drastic change in morphology of the transduced cells, where *SMARCA4* knockdown cells budded off (Figure 5A, i) and detached, followed by formation of spheres floating in suspension (Figure 5A, ii), which we also observed with another *SMARCA4* targeting shRNA (Figure S4). To investigate whether this phenotype can also be observed after chemical inhibition of SMARCA4, we treated NSCs with PFI-3 (Gerstenberger et al., 2016; Vangamudi et al., 2015). PFI-3 is a small-molecule inhibitor that specifically targets the bromodomain of family VIII bromodomain proteins, including SMARCA4, BRM, and BAF180 subunit of the SWI/SNF complex (Wu et al., 2017). Interestingly, treatment of NSCs with low μM concentrations of the drug led to similar phenotypes as observed after SMARCA4 knockdown (Figures 5B and S5). Nevertheless, because PFI-3 also binds to bromodomains of additional proteins, and because reports have shown that the bromodomain can be dispensable for essential functions of SMARCA4 (Vangamudi et al., 2015), further studies are required to investigate the drug-phenotype relationship.

To decipher *SMARCA4*'s role in NSC self-renewal and differentiation, we opted for examining the spheres formed by PFI-3 treatment due to its general affectivity compared with transducing only a proportion of cells. Staining of spherical sections of various sizes revealed a reduction or complete loss of NSC-specific marker expression

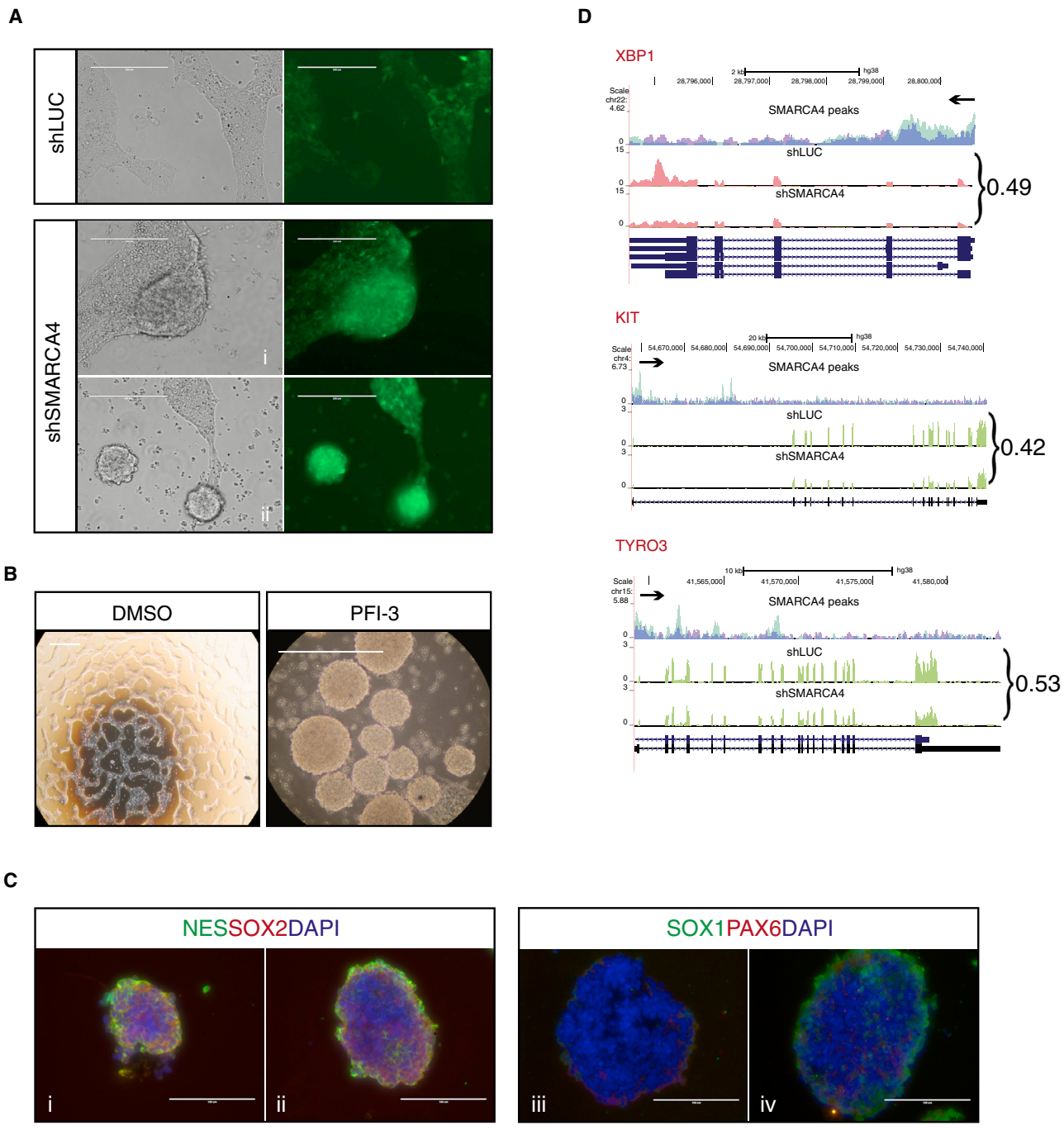

Figure 5. *SMARCA4* Depletion or Inhibition Causes Cell Detachment and Impedes Self-Renewal

(A) Change in morphology upon shSMARCA4 treatment. The bright-field (left) and fluorescent panels (right; exhibiting the infected cells in green) are shown. Control-treated cells (shLUC) grow as a monolayer (upper panel). The rounding up of the monolayer cells (i) upon SMARCA4 knockdown (shSMARCA4) followed by budding off into suspension (ii) phenotype is shown.

(B) The SMARCA4 inhibitor PFI-3 phenocopies neurosphere-like formation. Images of control (DMSO)- and 10 μM PFI-3-treated cells are shown.

(C) Immunofluorescence staining on cryo-sections of PFI-3-treated spheres. i–iv represent sections from different spheres. Marker-proteins for self-renewing NSCs (NES, SOX1, SOX2, and PAX6) are stained by antibodies in the colors indicated. DAPI staining is shown in blue. Scale bars, 200 μm (A and B), 100 μm (C).

(legend continued on next page)

(Figure 5C); suggesting loss of stemness. Collectively, sphere formation and loss of self-renewal explain *SMARCA4* depletion in the NSC-RNAi screen.

SMARCA4 Loss-Induced Downregulation of Adherence and Neural Suppressor Genes Can Be Reversed by *SMARCA4* Overexpression

SMARCA4 has been shown to act both as a transcriptional activator as well as a repressor (Attanasio et al., 2014). Because we observed the budding off phenotype, we hypothesized that cell adherence genes might be regulated by SMARCA4. Indeed, inspection of RNA-seq and chromatin immunoprecipitation sequencing (ChIP-seq) data performed on control and *SMARCA4* knockdown NSCs revealed that expression of several adherence genes are prominently changing on *SMARCA4* depletion (Figure S6). Expression of these genes, such as *XBP1*, *KIT*, and *TYRO3* (Figure 5D; Table S3) was downregulated upon *SMARCA4* knockdown, which possibly contributes to sphere formation. This finding also supports the role of SMARCA4 in extracellular matrix composition, in line with two previous reports (Barutcu et al., 2016; Saladi et al., 2010).

Genome-wide ChIP-seq analysis revealed that SMARCA4 tends to bind in the vicinity of transcription start sites (TSSs) (Figure 6A), and integrative analyses of the ChIP-seq with the RNA-seq data suggests that SMARCA4, at TSSs, acts both as a transcriptional activator as well as a repressor, supporting a previous study (Attanasio et al., 2014) (Figure 6B).

To investigate the depletion phenotype further, we assessed the differentiation capacity of NSCs upon *SMARCA4* knockdown by looking closely at the differentially expressed genes that are regulated by SMARCA4 and are involved in NSC self-renewal or differentiation. Among the promoters SMARCA4 binds to, we identified *RE-1-silencing transcription factor* (*REST*), a repressor of neuronal differentiation, and *ACTL6B* (*BRG-1-associated factor 53 [BAF53]*) (Figure S6). The BAF complex plays an important role during neural differentiation (Narayanan and Tuoc, 2014) and certain subunits are exchanged during differentiation. BAF53A is present in the neural progenitor BAF (npBAF) complex, whereas BAF53B exists in the neural BAF (nBAF) version (Lessard et al., 2007). RNA-seq data show that expression of *REST* was downregulated, whereas *ACTL6B* was upregulated upon *SMARCA4* depletion (Figure 6C). These findings were confirmed on protein level and, therefore, indicate that *SMARCA4* loss leads to a switch from BAF53A to BAF53B (Figure 6D). These results also argue that SMARCA4, together with REST, acts as a suppressor of neural differentiation, and its downregulation result in exit from the self-renewing state with skewed neural differentiation.

However, these results do not answer whether loss of self-renewal is a downstream artifact of cell detachment followed by sphere formation or if it is directly regulated by *SMARCA4*. To this end, we aimed to investigate how expression of REST and BAF53A change upon *SMARCA4* overexpression. Interestingly, *SMARCA4* overexpression resulted in upregulation of REST by 2.7-fold and BAF53A by 2.1-fold (Figure 6E), suggesting that *SMARCA4* exerts a more direct role in stemness regulation through suppression of neuronal differentiation genes. Together, these data suggest that *SMARCA4* directly regulates NSC self-renewal by suppressing neural differentiation together with REST. Furthermore, because *SMARCA4* regulates cell adherence and NSC self-renewal independently of each other, these findings suggest that *SMARCA4* is a direct regulator of stemness in NSCs.

DISCUSSION

In humans, it has been challenging to study isogenic stem cells. The emergence of iPSCs and protocols deriving other cell types from them (Zhao et al., 2013), including somatic stem cells (Sabapathy and Kumar, 2016; Sugimura et al., 2017), have opened the possibility to investigate human isogenic stem cells *ex vivo*. In this study, we exploited these advances to phenotypically compare isogenic human stem cells, and to investigate common and specific factors used in stem cell homeostasis and differentiation in HSPCs and NSCs. Because other cell types can be derived from iPSCs by directed differentiation, we envision that this approach can be extended to other cell types.

Despite the fact that its functions are not well understood in HSPCs, *SMARCA4* has been shown to be important in hematopoiesis by regulating myeloid differentiation (Holloway et al., 2003; Vradii et al., 2006), as well as in B and T cell development in the lymphoid lineage (Bossen et al., 2015; Chi et al., 2002; Choi et al., 2012). NSCs

(D) Downregulation of adhesion-related genes upon *SMARCA4* knockdown. Comparative depiction of the SMARCA4 binding (top) and the gene expression levels in the control (middle) versus knockdown (bottom) sample at the respective locus. SMARCA4 binding peaks are depicted in light blue for the eluted sample and in dark blue for the control (input) sample. Black arrows indicate the direction of transcription. SMARCA4 binding and mRNA levels are shown for *XBP1*, *KIT*, and *TYRO3*. Note the binding of SMARCA4, particularly to TSS and the reduced expression of the genes upon *SMARCA4* depletion. Normalized read count ratios are depicted to the left of the respective shLUC versus shSMARCA4 mRNA tracks.
See also Figures S4–S6 and Table S3.

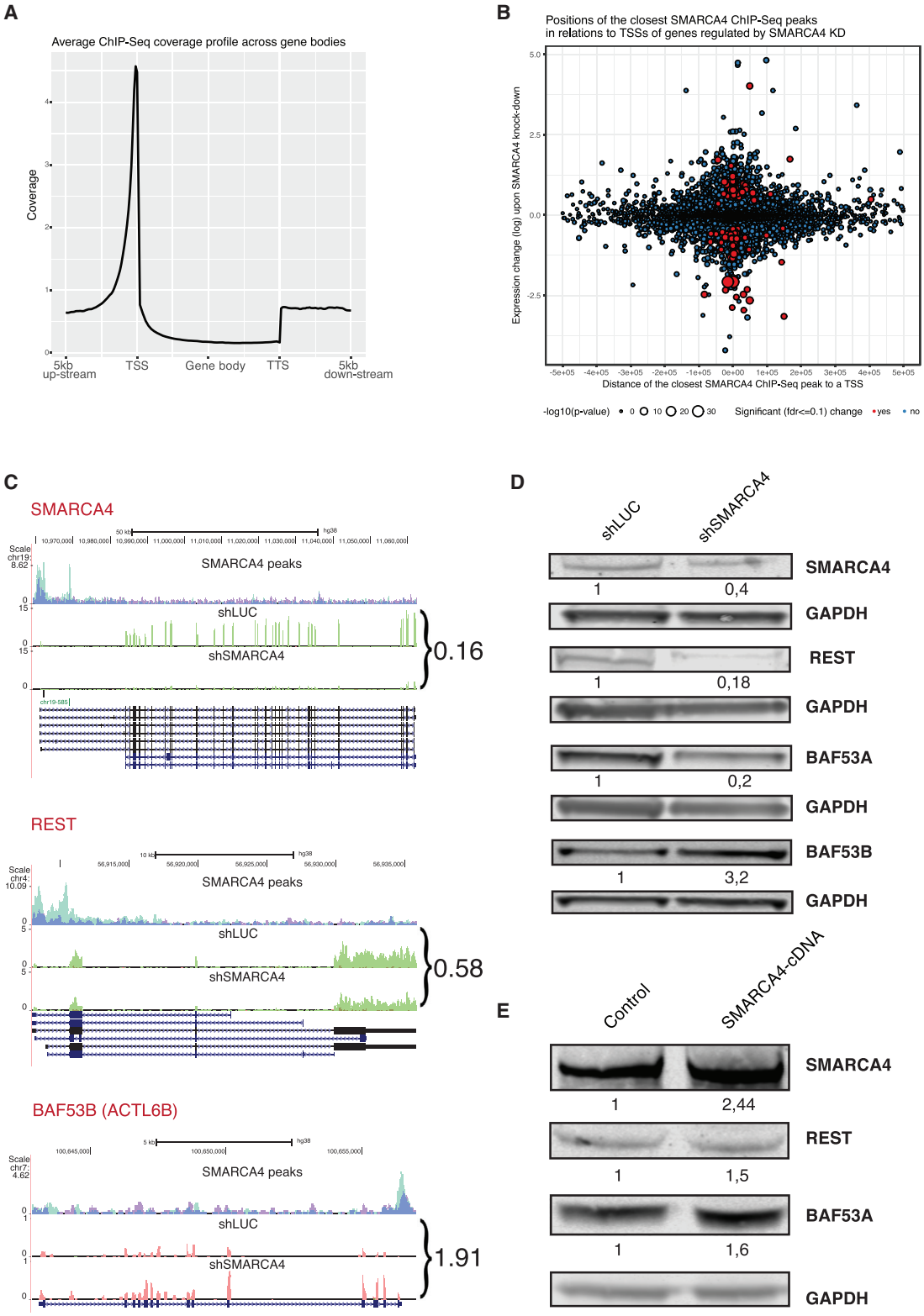

Figure 6. SMARCA4 De-represses Neuronal Genes

(A) SMARCA4 binding across genome spanning transcription start (TSS) and termination (TTS) sites, including 5 kb up- and downstream regions in NSCs.

(legend continued on next page)

have not been studied in humans to the same extent as in model organisms: *Smarca4* loss in mouse has been shown to result in fewer NSCs because of downregulation of self-renewal, and early neuronal differentiation before the onset of gliogenesis (Matsumoto et al., 2006). On the other hand, SMARCA4 is well characterized in hESCs, and was shown to be a direct regulator of pluripotency (Ho et al., 2009; Zhang et al., 2014). Therefore, in our study we focused on characterizing *SMARCA4* in depth in these two adult stem cell types, HSPCs and NSCs.

HSPCs set the starting point of our study, which we derived from easily accessible PB. For practical reasons, we used the widely applied marker CD34 to enrich for this cell population. However, sorting for CD34 is not sufficient to separate hematopoietic stem cells from progenitors. Intriguingly, we were able to distinguish these two populations during our validation experiments. After having validated the enrichment phenotype by showing the expansion of the $CD34^+$ population (increased cell number also in LTC-IC assay), a closer look at different hematopoietic subsets that are immunophenotypically similar to HSCs, MPPs, CLPs, and CMPs, revealed that HSCs as well as MPP are actually depleted upon *SMARCA4* knockdown; whereas CLP and CMP populations are enriched. *In vivo* data correlated with this finding, reflected by the reduced engraftment due to impaired self-renewal of LT-HSCs. These results indicate that the $CD34^+$ enrichment phenotype was due to an increase in the primed-progenitor population, and not in the stem cells. In the future, further analyses of downstream effects upon SMARCA4 depletion in HSCs, such as chromatin and gene expression changes, will be interesting, but might be challenging to obtain due to currently limited ability to expand these cells in culture.

To specifically screen for genes that more directly affect HSC behavior, one could employ additional markers during the sorting process, such as CD90, CD49f, and EMCN (endomucin) (Knapp et al., 2018; Notta et al., 2011; Reckzeh et al., 2018; Wisniewski et al., 2011). However, it might be difficult to obtain enough cells to ensure full coverage of large shRNA libraries. Reducing the library size by restricting the gene count or by only using previously validated silencing triggers might make this experiment feasible.

An interesting observation was that, in the CFU assay, assessing the clonogenic potential into myeloid lineage, the *SMARCA4* knockdown sample showed a 3-fold reduction in total colony numbers. Moreover, all emerging colonies were of the same type: CFU-GM. Supporting an earlier report, no erythroid colony formation was observed (Lee et al., 1999). These results suggest that *SMARCA4* knockdown traps CMP at the progenitor state and causes partial myeloid lineage specification (Holloway et al., 2003; Vradii et al., 2006). Future studies should address at which stage *SMARCA4* blocks differentiation from CMP to specified myeloid cells. Last but not least, it would be worth investigating *SMARCA4* functions in lymphoid lineage and whether a similar blockage occurs in CLP as well.

The role of SMARCA4 has been described in various mechanisms in hNSCs, including cell adherence (Barutcu et al., 2016; Saladi et al., 2010). In addition, a regulatory role in transcription has also been described for SMARCA4: SMARCA4 binds and acts synergistically with REST, a zinc-finger transcription factor. REST represses its target genes by recruiting its corepressors. Its reduced activity results in expression of neural genes, implying that SMARCA4 is involved in repressing neuronal-specific genes (Ooi et al., 2006). Our results reveal that the promoter of *REST* is bound by SMARCA4, and that REST expression gets downregulated upon *SMARCA4* knockdown. Hence, SMARCA4 might directly regulate the expression of REST to repress neuronal differentiation. Downregulation of BAF53A and concomitant upregulation of BAF53B provide evidence for exit from self-renewal and commitment to the neural lineage. cDNA-mediated overexpression elucidates a direct link for SMARCA4's involvement in self-renewal maintenance and indicates that neuronal differentiation upon *SMARCA4* knockdown is not an artifact of cell detachment. Last, but not least, it would be interesting to investigate the

(B) Positions of the SMARCA4 binding sites (peaks) in relation to TSS of genes regulated by SMARCA4. Expression change upon knockdown (y axis) versus distance of the closest SMARCA4 peak (x axis) is depicted. Significant expression change is shown in red (blue, not significant).

(C) Comparative depiction of the SMARCA4 binding (top) and the gene expression levels in the control (middle) versus SMARCA4 knockdown (bottom) samples at the respective locus. SMARCA4 binding peaks are depicted in light blue for the eluted sample and in dark blue for the control (input) sample. Black arrows indicate the direction of transcription. SMARCA4 binding and mRNA levels are depicted for *SMARCA4*, *REST*, and *ACTL6B* (*BAF53*B). Normalized read-count ratios are depicted to the right of the respective shLUC versus shSMARCA4 mRNA tracks. Note the reduced and increased expression of *REST* and *BAF53*B upon *SMARCA4* depletion, respectively.

(D) Protein levels of SMARCA4, REST, BAF53A, and BAF53B upon *SMARCA4* knockdown. Protein levels were normalized to GAPDH and shLUC control. Quantifications, normalized to the shLUC control are presented below the gels.

(E) Protein levels of SMARCA4, REST, and BAF53A upon *SMARCA4* overexpression. Protein levels were normalized to GAPDH and the control sample. Relative band intensity values are quantified below the western blots.

See also Figures S5 and S6 and Table S3.

interaction partners of the SMARCA4-REST complex and their target genes.

Previous studies in hESCs have shown SMARCA4 to be the only catalytic subunit of a specific SWI/SNF complex, namely ESC-BAF (esBAF) (Ho et al., 2009). This complex has a unique combinatorial assembly and harbors BAF60B, which only exists within esBAF. In this study, we have not addressed the composition of the BAF complex in hiPSCs. Thus, it would be interesting to investigate the BAF complex composition in iPSCs, to evaluate the degree of similarity to esBAF, and its adaptation upon differentiation. Therefore, future studies aiming to gain a deeper understanding of transcriptional modifications due to combinatorial BAF subunit assembly would be of interest.

In summary, we found that *SMARCA4* not only regulates self-renewal in isogenic HSPCs and NSCs, but also ensures a balanced lineage specification, in a fashion unique to the cell type. SMARCA4, as a chromatin remodeler involved in numerous regulations as a transcriptional activator and repressor, poses an interesting candidate for deciphering the balance between self-renewal and differentiation at a broad range of stem cells. Finally, although our approach reflects results from only a single individual, we show that comparative RNAi screens on isogenic human stem cells are feasible and, hence, a promising approach to identify regulators of stemness and differentiation.

EXPERIMENTAL PROCEDURES

The list of all antibodies used in this study are listed in Table S4, and primer sequences can be found in Tables S5 and S6.

Immunofluorescence Staining of PFI-3-Treated NSCs

NSCs were treated with 10 μM PFI-3 or DMSO control for 5 days. Neurospheres were pelleted for 1 min at 300 × *g*, and fixed with 4% PFA for 10 min at room temperature. Fixed samples were pelleted at 8,000 rpm for 15 s, embedded in 300–500 μL tissue embedding medium, OCT (Slee Medical) overnight at 4°C. Cryosectioning was performed in 8-μm-thick sections with an NX70 cryostat (Thermo Scientific) at −19°C. Sections were immunofluorescence stained with the hNSC immunocytochemistry kit (Thermo Scientific) according to the manufacturer's instructions. Images were acquired with an EVOS FL fluorescence microscope (Thermo Scientific) and analyzed using ImageJ image processing software.

Lentiviral Pooled shRNA Screens

A custom-made DECIPHER shRNA library (Cellecta) was used for all the RNAi screens. To reach 150-fold coverage, 5 million $CD34^+$ HSPCs and NSCs were transduced at an MOI of 0.3; ensuring that most transduced cells received a single shRNA copy. To select for the shRNA carrying stem cell population, cells were sorted, at each time point, based on the shRNA reporter marker combined with CD34 (HSPC) expression (95% of NSCs were $NESTIN^+SOX2^+$, therefore, not sorted). PCR-amplified gDNA carrying the shRNA barcodes was sequenced on a HiSeq 2500 Illumina sequencer. Samples were 75-bp single-end sequenced in packages of 8 samples per lane, at a depth of 30 million reads. Obtained counts of reads per shRNA were converted, for each sample individually, to logarithms of the odds ratios. Subsequently, they were converted into standard scores (*Z* scores), where for centering and scaling, means and standard deviations of log odd ratios associated with shRNAs targeting LUC control were used. To combine *Z* scores associated with shRNAs targeting the same gene, a trimmed mean was calculated with 15% as a trimming factor. In the case of genes targeted by 12 shRNAs, the 2 most extreme results were removed from each end before calculating a mean *Z* score.

Work with primary HSPCs was performed according to a positive vote from the local ethics committee (EK 363112012).

Lentiviral Transductions for Validation

HSPCs and NSCs were transduced (as described previously by Camgoz et al., 2018) at an MOI of 1. Transduced cells were further cultured or analyzed by flow cytometry based on GFP expression.

Plasmids

shRNA sequences were cloned and expressed as previously described (Camgoz et al., 2018). Constructs were confirmed by DNA sequencing.

Transfection

NSCs were transfected with the SMARCA4 expression construct pcDNA6.2/N-EmGFP-DEST (Addgene, no. 65391) using the C-13 program with Basic Primary Neurons Nucleofector Kit (Lonza) at a Nucleofector 2b Device (Lonza).

Quantitative Real-Time PCR

mRNA extraction was done as described previously (Camgoz et al., 2018). qPCR was performed using the ABsolute qPCR 2x SYBR Green Kit (Thermo Scientific) following the manufacturer's protocol on a CFX96 Real-Time System (Bio-Rad). Using the 2-ΔΔCt method, mRNA levels were normalized to the LUC control against GAPDH as an internal control.

LTC-IC

For the LTC-IC assay, $CD34^+$ HSPCs were transduced with *SMARCA4* and control shRNAs, and were subjected to 2 μg/mL puromycin selection between 2 and 4 dpt. A total of 1,000 cells/well were seeded on irradiated M2-10B4 murine BM stromal cells in a 96-well plate and cultured in MyeloCult H5100 (STEMCELL) according to the manufacturer's instructions (n = 5). Between week 2 and 5, cobblestones, defined as an area of at least five tightly adjacent hematopoietic cells with a rectangular shape, were manually counted using a Celigo cytometer (Brooks).

CFU Assay

$CD34^+$ HSPCs were transduced with *SMARCA4* and control shRNAs, and subjected to 2 μg/mL puromycin selection for 2 days. A total of 1,000 cells/dish were seeded in 3 replicates in

35-mm dishes with methylcellulose-containing medium supplemented with recombinant human stem cell factor, recombinant human GM-colony-stimulating factor (rhGM-CSF), rhG-CSF, recombinant human interleukin-3 (rhIL-3), rhIL-6, and recombinant human erythropoietin (MethoCult H4435 Enriched; STEMCELL). After 14 days, colony types and numbers were analyzed using a STEMvision instrument (STEMCELL).

Mice

NOD.Cg-*Prkdc*^{scid} *Il2rg*^{tm1Wjl}/SzJ *Kit*$^{W41/W41}$ mice (NSGW41) were generated by backcrossing the *Kit*^{W41} allele (C57BL/6-Kit < W-41 >) to NSG mice for 16 generations. The resulting heterozygous NSG *Kit*$^{W41/+}$ mice were intercrossed to receive the homozygous NSGW41 mice used for experiments (Cosgun et al., 2014). All mice were bred and maintained in individually ventilated cages under specific pathogen-free conditions at the experimental center of the TU Dresden. The Landesdirektion Dresden, as responsible authority, approved all animal experiments.

Transplantation

For humanization, 5 × 10^5 CD34-enriched cells were injected intravenously in 150 μL PBS/5% FCS into 7- to 11-week-old unconditioned NSGW41 mice. After transplantation mice were given neomycin-containing drinking water for 3 weeks.

Flow Cytometry Analysis and Cell Sorting

BM and blood samples were collected and prepared as described previously (Cosgun et al., 2014). Samples were acquired on an LSRII cytometer (BD Biosciences).

All other antibody stainings were performed according to the manufacturer's instructions. Samples were acquired in PBS-EB (0.5 M EDTA +0.4% [m/v] BSA in PBS) on a MACSQuant Analyzer (Miltenyi), FACSAria III sorter (BD Biosciences) or FACSCanto II SORP (BD Biosciences). Data were analyzed using FlowJo software (Tree Star).

ChIP-Seq

ChIP was done as described previously (Ding et al., 2015) using 20 μL of ChIP-grade SMARCA4. DNA was purified and eluted using a PCR purification kit (QIAGEN) in 30 μL HPLC-grade water. Samples were submitted to NGS on an Illumina HiSeq 2000. Gene expression levels were estimated with kallisto software (v.0.43.0), using cDNA sequences from Ensembl database (release 79) as a reference, and further differential expression analysis was performed using sleuth algorithm (v.0.28.1).

Data and Statistical Analysis

Data were analyzed using GraphPad Prism version 6 (GraphPad Software). Results were presented as SEM (presented as error bars). Comparisons between experimental groups were made using unpaired Student's two-tailed t test. $p < 0.05$ was considered to be statistically significant.

ACCESSION NUMBERS

The GEO accession number for the dataset of NGS, RNA-seq and ChIP-seq experiments reported in this paper is GEO: GSE125033.

SUPPLEMENTAL INFORMATION

Supplemental Information can be found online at https://doi.org/10.1016/j.stemcr.2019.03.012.

AUTHOR CONTRIBUTIONS

C.G. planned the research and executed the experiments. S.R. and C.W. performed the transplantation and bone marrow analysis. C.G. and M.P.-R. analyzed the data. S.K. performed the iPSC characterization experiments. A.C. performed the western blot of PFI-3 treatment, M.W. and M.B. contributed materials. A.D. performed the deep-sequencing experiments. C.G. and F.B. wrote the manuscript with input from all the authors.

ACKNOWLEDGMENTS

We would like to thank Katja Bernhardt and Anne Gompf from the Core Flow Cytometry for their help with the FACS analysis. The excellent help of Srimasorn Sumitra during NSC derivation is greatly acknowledged. We also thank all Buchholz laboratory members for their valuable feedback and discussions. The project was supported by grants from German Cancer Aid (Deutsche Krebshilfe, SyTASC/70111969) and the German Research Foundation (DFG) SFB655 (B5). C.W. was supported by the German Research Foundation (DFG) through FOR2033-A03, TRR127-A5, WA2837/6-1, and WA2837/7-1.

Received: December 4, 2018
Revised: March 26, 2019
Accepted: March 27, 2019
Published: April 25, 2019

REFERENCES

Akashi, K., Traver, D., Miyamoto, T., and Weissman, I.L. (2000). A clonogenic common myeloid progenitor that gives rise to all myeloid lineages. Nature *404*, 193–197.

Ali, N., Karlsson, C., Aspling, M., Hu, G., Hacohen, N., Scadden, D.T., and Larsson, J. (2009). Forward RNAi screens in primary human hematopoietic stem/progenitor cells. Blood *113*, 3690–3695.

Attanasio, C., Nord, A.S., Zhu, Y., Blow, M.J., Biddie, S.C., Mendenhall, E.M., Dixon, J., Wright, C., Hosseini, R., Akiyama, J.A., et al. (2014). Tissue-specific SMARCA4 binding at active and repressed regulatory elements during embryogenesis. Genome Res. *24*, 920–929.

Barutcu, A.R., Lajoie, B.R., Fritz, A.J., McCord, R.P., Nickerson, J.A., van Wijnen, A.J., Lian, J.B., Stein, J.L., Dekker, J., Stein, G.S., et al. (2016). SMARCA4 regulates gene expression and higher-order chromatin structure in proliferating mammary epithelial cells. Genome Res. *26*, 1188–1201.

Baudet, A., Karlsson, C., Safaee Talkhoncheh, M., Galeev, R., Magnusson, M., and Larsson, J. (2012). RNAi screen identifies MAPK14 as a druggable suppressor of human hematopoietic stem cell expansion. Blood *119*, 6255–6258.

Bossen, C., Murre, C.S., Chang, A.N., Mansson, R., Rodewald, H.-R., and Murre, C. (2015). The chromatin remodeler Brg1

activates enhancer repertoires to establish B cell identity and modulate cell growth. Nat. Immunol. *16*, 775–784.

Camgoz, A., Paszkowski-Rogacz, M., Satpathy, S., Wermke, M., Hamann, M.V., von Bonin, M., Choudhary, C., Knapp, S., and Buchholz, F. (2018). STK3 is a therapeutic target for a subset of acute myeloid leukemias. Oncotarget *9*, 25458–25473.

Chi, T.H., Wan, M., Zhao, K., Taniuchi, I., Chen, L., Littman, D.R., and Crabtree, G.R. (2002). Reciprocal regulation of CD4/CD8 expression by SWI/SNF-like BAF complexes. Nature *418*, 195–199.

Choi, J., Ko, M., Jeon, S., Jeon, Y., Park, K., Lee, C., Lee, H., and Seong, R.H. (2012). The SWI/SNF-like BAF complex is essential for early B cell development. J. Immunol. *188*, 3791–3803.

Chu, L.-F., Leng, N., Zhang, J., Hou, Z., Mamott, D., Vereide, D.T., Choi, J., Kendziorski, C., Stewart, R., and Thomson, J.A. (2016). Single-cell RNA-seq reveals novel regulators of human embryonic stem cell differentiation to definitive endoderm. Genome Biol. *17*, 173.

Cosgun, K.N., Rahmig, S., Mende, N., Reinke, S., Hauber, I., Schäfer, C., Petzold, A., Weisbach, H., Heidkamp, G., Purbojo, A., et al. (2014). Kit regulates HSC engraftment across the human-mouse species barrier. Cell Stem Cell *15*, 227–238.

Daley, G.Q., Goodell, M.A., and Snyder, E.Y. (2003). Realistic prospects for stem cell therapeutics. Hematology Am. Soc. Hematol. Educ. Program, 398–418.

Ding, L., Paszkowski-Rogacz, M., Winzi, M., Chakraborty, D., Theis, M., Singh, S., Ciotta, G., Poser, I., Roguev, A., Chu, W.K., et al. (2015). Systems analyses reveal shared and diverse attributes of Oct4 regulation in pluripotent cells. Cell Syst. *1*, 141–151.

Ding, L., Poser, I., Paszkowski-Rogacz, M., and Buchholz, F. (2011). From RNAi screens to molecular function in embryonic stem cells. Stem Cell Rev. Rep. *8*, 32–42.

Elling, U., and Penninger, J.M. (2014). Genome wide functional genetics in haploid cells. FEBS Lett. *588*, 2415–2421.

Fares, I., Chagraoui, J., Gareau, Y., Gingras, S., Ruel, R., Mayotte, N., Csaszar, E., Knapp, D.J.H.F., Miller, P., Ngom, M., et al. (2014). Cord blood expansion. Pyrimidoindole derivatives are agonists of human hematopoietic stem cell self-renewal. Science *345*, 1509–1512.

Fares, I., Chagraoui, J., Lehnertz, B., MacRae, T., Mayotte, N., Tomellini, E., Aubert, L., Roux, P.P., and Sauvageau, G. (2017). EPCR expression marks UM171-expanded CD34(+) cord blood stem cells. Blood *129*, 3344–3351.

Galeev, R., Baudet, A., Kumar, P., Rundberg Nilsson, A., Nilsson, B., Soneji, S., Törngren, T., Borg, Å., Kvist, A., and Larsson, J. (2016). Genome-wide RNAi screen identifies cohesin genes as modifiers of renewal and differentiation in human HSCs. Cell Rep. *14*, 1–13.

Gerstenberger, B.S., Trzupek, J.D., Tallant, C., Fedorov, O., Filippakopoulos, P., Brennan, P.E., Fedele, V., Martin, S., Picaud, S., Rogers, C., et al. (2016). Identification of a chemical probe for family VIII bromodomains through optimization of a fragment hit. J. Med. Chem. *59*, 4800–4811.

Ho, L., Ronan, J.L., Wu, J., Staahl, B.T., Chen, L., Kuo, A., Lessard, J., Nesvizhskii, A.I., Ranish, J., and Crabtree, G.R. (2009). An embryonic stem cell chromatin remodeling complex, esBAF, is essential for embryonic stem cell self-renewal and pluripotency. Proc. Natl. Acad. Sci. U S A *106*, 5181–5186.

Holloway, A.F., Rao, S., Chen, X., and Shannon, M.F. (2003). Changes in chromatin accessibility across the GM-CSF promoter upon T cell activation are dependent on nuclear factor kappaB proteins. J. Exp. Med. *197*, 413–423.

Keller, G. (2005). Embryonic stem cell differentiation: emergence of a new era in biology and medicine. Genes Dev. *19*, 1129–1155.

Knapp, D.J.H.F., Hammond, C.A., Hui, T., Loenhout, M.T.J., Wang, F., Aghaeepour, N., Miller, P.H., Moksa, M., Rabu, G.M., Beer, P.A., et al. (2018). Single-cell analysis identifies a CD33+ subset of human cord blood cells with high regenerative potential. Nat. Cell Biol. *20*, 710–720.

Kondo, M., Weissman, I.L., and Akashi, K. (1997). Identification of clonogenic common lymphoid progenitors in mouse bone marrow. Cell *91*, 661–672.

Lee, C.H., Murphy, M.R., Lee, J.S., and Chung, J.H. (1999). Targeting a SWI/SNF-related chromatin remodeling complex to the beta-globin promoter in erythroid cells. Proc. Natl. Acad. Sci. U S A *96*, 12311–12315.

Lessard, J., Wu, J.I., Ranish, J.A., Wan, M., Winslow, M.M., Staahl, B.T., Wu, H., Aebersold, R., Graef, I.A., and Crabtree, G.R. (2007). An essential switch in subunit composition of a chromatin remodeling complex during neural development. Neuron *55*, 201–215.

MacRae, T., Sargeant, T., Lemieux, S., Hébert, J., Deneault, É., and Sauvageau, G. (2013). RNA-seq reveals spliceosome and proteasome genes as most consistent transcripts in human cancer cells. PLoS One *8*, e72884–e72889.

Matsumoto, S., Banine, F., Struve, J., Xing, R., Adams, C., Liu, Y., Metzger, D., Chambon, P., Rao, M.S., and Sherman, L.S. (2006). Brg1 is required for murine neural stem cell maintenance and gliogenesis. Dev. Biol. *289*, 372–383.

Moffat, J., and Sabatini, D.M. (2006). Building mammalian signalling pathways with RNAi screens. Nat. Rev. Mol. Cell Biol. *7*, 177–187.

Narayanan, R., and Tuoc, T.C. (2014). Roles of chromatin remodeling BAF complex in neural differentiation and reprogramming. Cell Tissue Res. *356*, 575–584.

Notta, F., Doulatov, S., Laurenti, E., Poeppl, A., Jurisica, I., and Dick, J.E. (2011). Isolation of single human hematopoietic stem cells capable of long-term multilineage engraftment. Science *333*, 218–221.

Ooi, L., Belyaev, N.D., Miyake, K., Wood, I.C., and Buckley, N.J. (2006). BRG1 chromatin remodeling activity is required for efficient chromatin binding by repressor element 1-silencing transcription factor (REST) and facilitates REST-mediated repression. J. Biol. Chem. *281*, 38974–38980.

Orkin, S.H., and Zon, L.I. (2008). Hematopoiesis: an evolving paradigm for stem cell biology. Cell *132*, 631–644.

Pabst, C., Krosl, J., Fares, I., Boucher, G., Ruel, R., Marinier, A., Lemieux, S., Hébert, J., and Sauvageau, G. (2014). Identification of small molecules that support human leukemia stem cell activity ex vivo. Nat. Methods *11*, 436–442.

Peterson, C.L., and Tamkun, J.W. (1995). The SWI-SNF complex: a chromatin remodeling machine? Trends Biochem. Sci. *20*, 143–146.

Petzer, A.L., Hogge, D.E., Landsdorp, P.M., Reid, D.S., and Eaves, C.J. (1996). Self-renewal of primitive human hematopoietic cells (long-term-culture-initiating cells) in vitro and their expansion in defined medium. Proc. Natl. Acad. Sci. U S A *93*, 1470–1474.

Reckzeh, K., Kizilkaya, H., Helbo, A.S., Alrich, M.E., Deslauriers, A.G., Grover, A., Rapin, N., Asmar, F., Grønbæk, K., Porse, B., et al. (2018). Human adult HSCs can be discriminated from lineage-committed HPCs by the expression of endomucin. Blood Adv. *2*, 1628–1632.

Reinhardt, P., Glatza, M., Hemmer, K., Tsytsyura, Y., Thiel, C.S., Höing, S., Moritz, S., Parga, J.A., Wagner, L., Bruder, J.M., et al. (2013). Derivation and expansion using only small molecules of human neural progenitors for neurodegenerative disease modeling. PLoS One *8*, e59252.

Sabapathy, V., and Kumar, S. (2016). hiPSC-derived iMSCs: NextGen MSCs as an advanced therapeutically active cell resource for regenerative medicine. J. Cell. Mol. Med. *20*, 1571–1588.

Saladi, S.V., Keenen, B., Marathe, H.G., Qi, H., Chin, K.-V., and de la Serna, I.L. (2010). Modulation of extracellular matrix/adhesion molecule expression by BRG1 is associated with increased melanoma invasiveness. Mol. Cancer *9*, 280.

Sugimura, R., Jha, D.K., Han, A., Soria-Valles, C., da Rocha, E.L., Lu, Y.-F., Goettel, J.A., Serrao, E., Rowe, R.G., Malleshaiah, M., et al. (2017). Haematopoietic stem and progenitor cells from human pluripotent stem cells. Nature *545*, 432–438.

Takahashi, K., and Yamanaka, S. (2006). Induction of pluripotent stem cells from mouse embryonic and adult fibroblast cultures by defined factors. Cell *126*, 663–676.

Takahashi, K., Tanabe, K., Ohnuki, M., Narita, M., Ichisaka, T., Tomoda, K., and Yamanaka, S. (2007). Induction of pluripotent stem cells from adult human fibroblasts by defined factors. Cell *131*, 861–872.

Trotter, K.W., and Archer, T.K. (2008). The BRG1 transcriptional coregulator. Nucl. Recept. Signal. *6*, e004.

Vangamudi, B., Paul, T.A., Shah, P.K., Kost-Alimova, M., Nottebaum, L., Shi, X., Zhan, Y., Leo, E., Mahadeshwar, H.S., Protopopov, A., et al. (2015). The SMARCA2/4 ATPase domain surpasses the bromodomain as a drug target in SWI/SNF-mutant cancers: insights from cDNA rescue and PFI-3 inhibitor studies. Cancer Res. *75*, 3865–3878.

Vradii, D., Wagner, S., Doan, D.N., Nickerson, J.A., Montecino, M., Lian, J.B., Stein, J.L., van Wijnen, A.J., Imbalzano, A.N., and Stein, G.S. (2006). Brg1, the ATPase subunit of the SWI/SNF chromatin remodeling complex, is required for myeloid differentiation to granulocytes. J. Cell. Physiol. *206*, 112–118.

Wermke, M., Camgoz, A., Paszkowski-Rogacz, M., Thieme, S., von Bonin, M., Dahl, A., Platzbecker, U., Theis, M., Ehninger, G., Brenner, S., et al. (2015). RNAi profiling of primary human AML cells identifies ROCK1 as a therapeutic target and nominates fasudil as an antileukemic drug. Blood *125*, 3760–3768.

Wisniewski, D., Affer, M., Willshire, J., and Clarkson, B. (2011). Further phenotypic characterization of the primitive lineage−CD34+CD38−CD90+CD45RA−hematopoietic stem cell/progenitor cell sub-population isolated from cord blood, mobilized peripheral blood and patients with chronic myelogenous leukemia. Blood Cancer J. *1*, e36–11.

Wu, Q., Lian, J.B., Stein, J.L., Stein, G.S., Nickerson, J.A., and Imbalzano, A.N. (2017). The BRG1 ATPase of human SWI/SNF chromatin remodeling enzymes as a driver of cancer. Epigenomics *9*, 919–931.

Yu, J., Vodyanik, M.A., Smuga-Otto, K., Antosiewicz-Bourget, J., Frane, J.L., Tian, S., Nie, J., Jonsdottir, G.A., Ruotti, V., Stewart, R., et al. (2007). Induced pluripotent stem cell lines derived from human somatic cells. Science *318*, 1917–1920.

Zhang, X., Li, B., Li, W., Ma, L., Zheng, D., Li, L., Yang, W., Chu, M., Chen, W., Mailman, R.B., et al. (2014). Transcriptional repression by the BRG1-SWI/SNF complex affects the pluripotency of human embryonic stem cells. Stem Cell Reports *3*, 460–474.

Zhao, J., Jiang, W.-J., Sun, C., Hou, C.-Z., Yang, X.-M., and Gao, J.-G. (2013). Induced pluripotent stem cells: origins, applications, and future perspectives. J. Zhejiang Univ. Sci. B *14*, 1059–1069.

Zon, L.I. (2008). Intrinsic and extrinsic control of haematopoietic stem-cell self-renewal. Nature *453*, 306–313.